J Mater Sci (2010) 45:919–928
DOI 10.1007/s10853-009-4021-7

Kinetics of reactive diffusion between Ta and Cu–9.3Sn–0.3Ti alloy

Y. Tejima · S. Nakamura · M. Kajihara

Received: 15 July 2009 / Accepted: 5 November 2009 / Published online: 21 November 2009

Abstract Tantalum is used as a diffusion barrier in the superconducting Nb_3Sn composite-wire manufactured by the bronze method. In order to examine the consumption behavior of the Ta barrier during annealing in the bronze method, the kinetics of the reactive diffusion between Ta and a bronze was experimentally observed using sandwich diffusion couples composed of Ta and a Cu–9.3Sn–0.3Ti alloy. The (Cu–Sn–Ti)/Ta/(Cu–Sn–Ti) diffusion couples were isothermally annealed at temperatures of $T = 973$–1053 K for various times up to $t = 1462$ h. Owing to annealing, Ta_9Sn is formed as a uniform layer at the initial (Cu–Sn–Ti)/Ta interface in the diffusion couple, and gradually grows mainly toward Ta. The mean thickness of the Ta_9Sn layer is proportional to a power function of the annealing time. However, the exponent of the power function is equal to unity at $t < t_c$ but smaller than 0.5 at $t > t_c$. Thus, the transition of the rate-controlling process for the growth of Ta_9Sn occurs at $t = t_c$. The critical annealing time t_c takes values of 1.83×10^6, 4.63×10^5, and 5.98×10^5 s at $T = 973$, 1023, and 1053 K, respectively. The growth of Ta_9Sn is controlled by the interface reaction at the migrating Ta_9Sn/Ta interface in the early stages with $t < t_c$ but by the volume and boundary diffusion across the Ta_9Sn layer in the late stages with $t > t_c$. Due to the transition of the rate-controlling process, the growth rate is always much smaller for Ta_9Sn than for Nb_3Sn. As a result, Ta works as an effective barrier against the diffusion of Sn from the bronze to the Cu stabilizer in the superconducting Nb_3Sn composite-wire.

Y. Tejima · S. Nakamura · M. Kajihara (✉)
Department of Materials Science and Engineering, Graduate School, Tokyo Institute of Technology, Yokohama 226-8502, Japan
e-mail: kajihara@materia.titech.ac.jp

Introduction

A bronze method has been conveniently used to manufacture superconducting Nb_3Sn composite-wires with multifilamentary structure [1–12]. Here, Nb_3Sn is an intermetallic compound with the A-15 type crystal structure. In the bronze method, a ductile rod of Nb is embedded in a Cu–Sn alloy matrix and then extruded into a filament form. A bundle of filaments are inserted into a Ta tube covered with a Cu tube and then extruded into a wire. The resultant multifilamentary wire is annealed at an appropriate temperature. Due to reactive diffusion during annealing, a Nb_3Sn layer is formed at the interface between the Cu–Sn alloy and Nb. The Cu–Sn alloy is denominated bronze, and hence this technique is called the bronze method. In the bronze method, the Cu tube works as a stabilizer of electric current, and the Ta tube acts as a diffusion barrier against the penetration of Sn into the Cu stabilizer from the bronze during annealing. The growth behavior of the Nb_3Sn layer in the bronze method was investigated by many researchers [5–12]. However, monofilamentary and multifilamentary diffusion couples were adopted in most of the investigations. In such diffusion couples, interdiffusion is complicated, and hence the Nb_3Sn layer with a uniform thickness cannot be formed easily. Consequently, the filamentary diffusion couples are not adequate to observe the growth behavior of the Nb_3Sn layer.

Instead of the filamentary diffusion couples, sandwich (Cu–Sn)/Nb/(Cu–Sn) diffusion couples were used to study experimentally the growth behavior of the Nb_3Sn layer in the bronze method [13, 14]. In the sandwich diffusion couple, interdiffusion takes place along the direction perpendicular to the initial (Cu–Sn)/Nb interface, and thus the Nb_3Sn layer with a uniform thickness is formed during the

interdiffusion. In the experiment by Osamura et al. [13], sandwich diffusion couples were prepared from Nb and a binary Cu–Sn alloy containing 7.4 at.% of Sn, and then isothermally annealed in the temperature range of $T = 973$–1073 K. On the other hand, in a previous study [14], sandwich diffusion couples composed of Nb and a binary Cu–8.3Sn alloy were isothermally annealed at $T = 923$–1053 K. In order to improve the superconducting properties of Nb_3Sn, a small amount of Ti is added into the Cu–Sn alloy. The influence of Ti on the growth of Nb_3Sn was experimentally studied by Osamura et al. [13] at $T = 973$–1073 K using (Cu–7.5Sn–1Ti)/Nb/(Cu–7.5Sn–1Ti) diffusion couples. The influence of Ti was also experimentally examined at $T = 923$–1053 K using sandwich diffusion couples consisting of Nb and a Cu–8.1Sn–0.3Ti alloy in a previous study [15]. According to these experiments [13, 15], the addition of Ti into the Cu–Sn alloy remarkably expedites the growth of Nb_3Sn at the higher annealing temperatures but hardly at the lower annealing temperatures.

Recently, Cu–Sn alloys with the $\alpha + \beta$ two-phase microstructure have been preferentially used to manufacture the superconducting Nb_3Sn composite-wire. Here, α is the primary solid-solution phase of Cu with the face-centered cubic structure, and β is the intermediate phase with the body-centered cubic structure. Since the concentration of Sn is higher in the β phase than in the α phase, the amount of Sn supplied to Nb_3Sn is greater for the Cu–Sn alloy with the $\alpha + \beta$ two-phase microstructure than for that with the α single-phase microstructure. Therefore, the influence of the β phase on the growth of Nb_3Sn was experimentally examined at $T = 923$–1053 K using sandwich diffusion couples composed of Nb and a Cu–9.3Sn–0.3Ti alloy in a previous study [16]. According to the experimental result, the growth rate is hardly affected by the volume fraction of the β phase, though the final amount of the Nb_3Sn layer depends on the volume fraction. According to the results in these experiments [13–16], the mean thickness of the Nb_3Sn layer is expressed as a power function of the annealing time, and the exponent of the power function is typically close to unity. This means that the growth of Nb_3Sn is predominantly controlled by the interface reaction.

As mentioned above, Ta is used as a barrier against the diffusion of Sn from the bronze to the Cu tube [17–19]. During annealing, however, a Ta–Sn compound may be formed as a layer at the interface between the Ta tube and the bronze due to the reactive diffusion and will grow to consume the Ta tube. When the consumption is completely finished, Sn penetrates into the Cu tube from the Ta–Sn compound. Such penetration deteriorates the electrical conductivity of the Cu tube and hence the stability of the composite-wire. Furthermore, the alternating current loss may be increased by the Ta–Sn compound layer, if the compound is the superconductive Ta_3Sn phase with the A-15 type crystal structure [20]. Unfortunately, no reliable metallographical information is available for the Ta–Sn compound formed by annealing in the bronze method. Thus, in a previous study [21], the reactive diffusion between Ta and a bronze with the $\alpha + \beta$ two-phase microstructure was experimentally observed at $T = 1053$ K using sandwich diffusion couples consisting of Ta and a Cu–9.3Sn–0.3Ti alloy. According to the observation, Ta_9Sn is produced at the (Cu–Sn–Ti)/Ta interface in the diffusion couple and gradually grows toward Ta. For the growth of Ta_9Sn, the transition of the rate-controlling process appears within the experimental annealing times. In order to examine whether Ta_9Sn is stable and the transition is realized in a wide temperature range, the reactive diffusion in the (Cu–Sn–Ti)/Ta system was extensively observed in the present study. The observation was performed at $T = 973$–1053 K using the same type of diffusion couple as a pervious study [21].

Experimental

Plate specimens with a dimension of $2 \times 5 \times 12$ mm^3 were prepared by spark erosion from a hot-rolled rectangular ingot of a ternary Cu–9.3Sn–0.3Ti alloy in a manner similar to a previous study [21]. Parallel surfaces with an area of 5×12 mm^2 of each Cu–Sn–Ti plate specimen were mechanically polished on 120–800 emery papers. One of the polished parallel-surfaces was again mechanically polished on 1500–4000 emery papers, and then finished using diamond with a size of 1 μm. Pure Ta sheet specimens with a dimension of $0.1 \times 5 \times 12$ mm^3 were degreased in acetone with an ultrasonic cleaner. After degreasing, a Ta-sheet specimen was immediately sandwiched between the finished surfaces of two freshly prepared Cu–Sn–Ti plate specimens in ethanol by the technique reported in a previous study [14]. Each sandwich couple was completely dried, and then isothermally heat-treated for diffusion bonding in an evacuated silica tube, followed by air-cooling. The diffusion bonding was carried out at temperatures of 973, 1023, and 1053 K for times of 48, 36, and 24 h, respectively. The diffusion couples were separately encapsulated in evacuated silica capsules, and then isothermally annealed at temperatures of 973, 1023, and 1053 K for various times up to 1414 h, followed by water-quenching without breaking the capsules. Hereafter, the summation of the heat-treating and annealing times is merely called the annealing time t, and the annealing temperature is denoted by T. Cross-sections of the annealed diffusion couple were mechanically polished using 1500–4000 emery papers and diamond with a size of 1 μm, and then finished with an OP–S liquid by Struers Ltd. The

microstructure of the cross-section was observed by optical microscopy (OM). The observation was also conducted with a backscattered electron image (BEI) by scanning electron microscopy (SEM). Concentration profiles of Cu, Sn, Ta, and Ti for various phases on the cross-section were measured by electron probe microanalysis (EPMA).

Results and discussion

Microstructure

A typical OM photograph for the cross-section of the annealed diffusion couple is shown in Fig. 1. This figure indicates the photograph for the diffusion couple with an annealing temperature of $T = 1053$ K and an annealing time of $t = 140$ h (5.04×10^5 s). In Fig. 1, the upper-side and lower-side regions are Ta and the Cu–Sn–Ti alloy, respectively. As can be seen, the Cu–Sn–Ti alloy consists of two phases with bright and dark contrasts. The bright and dark phases are the α and β phases, respectively. Here, α is the primary solid-solution phase of Cu with the face-centered cubic (fcc) structure, and β is the intermediate phase with the body-centered cubic (bcc) structure. According to the photograph in Fig. 1, the β phase is rather irregular in morphology. Furthermore, dendritic grains of the α phase are distributed in the β phase. On the other hand, a thin layer with a uniform thickness is formed between Ta and the Cu–Sn–Ti alloy. Concentration profiles of the constituent components across the thin layer were measured by EPMA. A typical result is shown in Fig. 2. In this figure, the ordinate and the abscissa indicate the mol fraction y_i of component i and the distance x, respectively, and open circles, squares, rhombuses, and triangles show the mol fractions

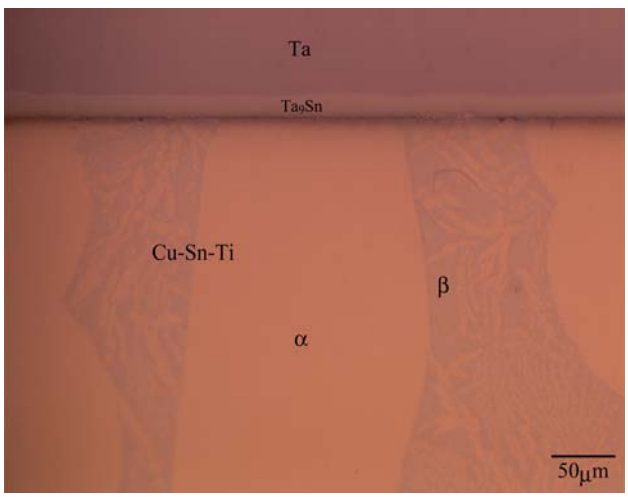

Fig. 1 OM photograph of cross-section for the diffusion couple annealed at $T = 1053$ K for $t = 140$ h (5.04×10^5 s)

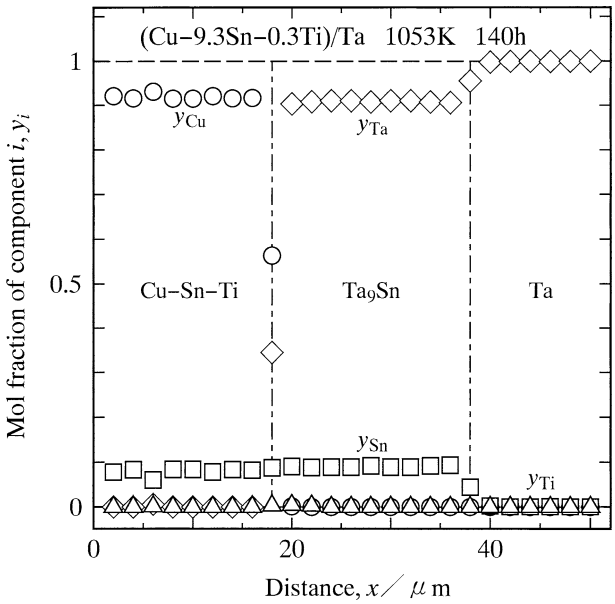

Fig. 2 Concentration profiles of Cu, Sn, Ta, and Ti across the Ta_9Sn layer in the diffusion couple shown in Fig. 1

y_{Cu}, y_{Sn}, y_{Ta}, and y_{Ti}, respectively. The EPMA measurement in Fig. 2 indicates that the thin layer between Ta and the Cu–Sn–Ti alloy is Ta_9Sn. The Ta_9Sn layer was recognized in all the diffusion couples annealed at $T = 973$–1053 K. Unfortunately, however, the thickness of the Ta_9Sn layer was merely 33 μm even after the longest annealing at $T = 1053$ K. Thus, the present diffusion couple was not appropriate for reliable identification of the crystal structure of Ta_9Sn by an X-ray diffraction technique. As can be seen in Fig. 2, the concentrations of Cu and Ti in Ta_9Sn are negligible. In contrast, the concentration of Sn is slightly greater in Ta_9Sn than in the α phase. Thus, the uphill diffusion of Sn occurs from the α phase to Ta_9Sn.

The concentration profiles in Fig. 2 are plotted as a diffusion path in the composition triangle of the ternary Cu–Sn–Ta system in Fig. 3. In this figure, open circles show the experimental points in Fig. 2, and open squares indicate the initial compositions of Ta and the Cu–Sn–Ti alloy. On the other hand, open rhombuses represent the equilibrium compositions of the α and β phases at $T = 1053$ K [22] and the stoichiometric composition of Ta_9Sn. As can be seen, the experimental composition of Ta_9Sn is close to the stoichiometric composition. Since both the α and β phases are directly contacted with Ta_9Sn in all the annealed diffusion couples as shown in Fig. 1, the $\alpha + \beta + Ta_9Sn$ three-phase equilibrium exists at $T = 973$–1053 K in the ternary Cu–Sn–Ta system. The tie-triangle of this three-phase equilibrium is indicated as solid lines in Fig. 3. In contrast, the phase equilibria in the binary Ta–Sn system were experimentally determined by Studnitzky and Schmid-Fetzer in the composition range of

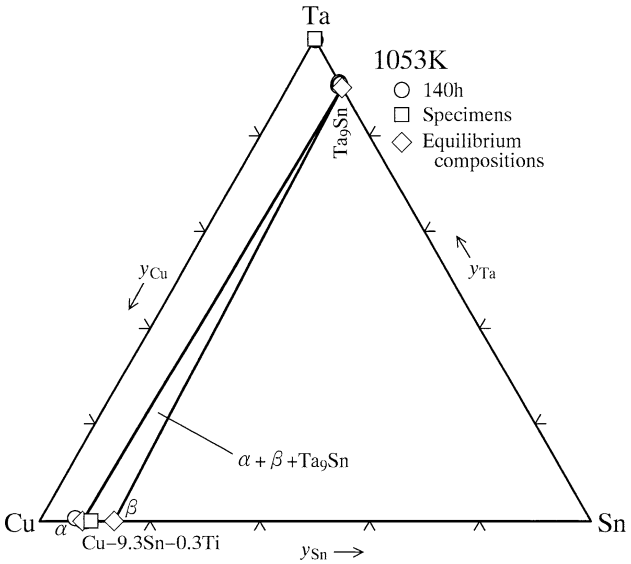

Fig. 3 Diffusion path for the concentration profile shown in Fig. 2

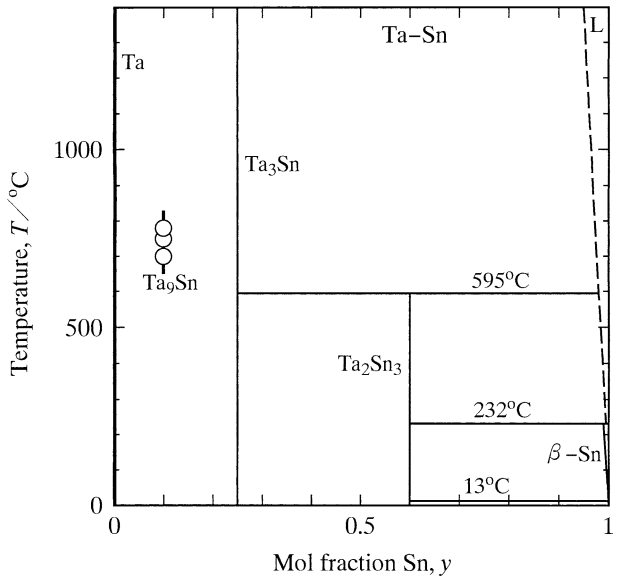

Fig. 4 Phase diagram in the binary Ta–Sn system reported by Studnitzky and Schmid-Fetzer [23]. *Open circles* show the annealing temperatures for formation of Ta_9Sn in the present study

$y_{Sn} = 0.25$–1 [23]. Their result is shown in Fig. 4. As can be seen, Ta_3Sn and Ta_2Sn_3 are stable compounds in the binary Ta–Sn system. Furthermore, Ta_2Sn_3 is formed by the peritectic reaction $L + Ta_3Sn \rightarrow Ta_2Sn_3$ at $T = 868$ K, where L stands for the liquid phase of Sn. According to the observation in the present study, Ta_9Sn arises as a stable compound at $T = 973$–1053 K as indicated with open circles in Fig. 4. Consequently, Ta_3Sn cannot be in equilibrium with Ta at $T = 973$–1053 K. However, no reliable information is available for the invariant reaction among Ta, Ta_9Sn, and Ta_3Sn.

Growth behavior of Ta_9Sn

In the OM photographs of the cross-section like Fig. 1, the Ta_9Sn layer is clearly distinguishable from Ta and the Cu–Sn–Ti alloy. Hence, from such OM photographs, the mean thickness l of the Ta_9Sn layer was evaluated as follows:

$$l = \frac{A}{w}. \tag{1}$$

Here, w and A are the total length parallel to the initial (Cu–Sn–Ti)/Ta interface and the total area of the Ta_9Sn layer, respectively, on the cross-section. The results of $T = 973$, 1023, and 1053 K are plotted as open rhombuses, squares, and circles, respectively, in Fig. 5. In this figure, the ordinate and the abscissa show the logarithms of l and t, respectively. As to $T = 1053$ K, the experimental reproducibility was confirmed between the observations in a previous study [21] and the present study. Hence, at $T = 1053$ K, only the result in a previous study [21] is shown as the open circles in Fig. 5. As can be seen, the thickness l monotonically increases with increasing annealing time t. Although the open squares for $T = 1023$ K are slightly scattered at longer annealing times, the open symbols are located well on straight lines with larger and smaller gradients at shorter and longer annealing times, respectively, at each annealing temperature. Hereafter, the stages at the shorter and longer annealing times are called stages I and II, respectively. In each stage, l is expressed as a power function of t by the following equation:

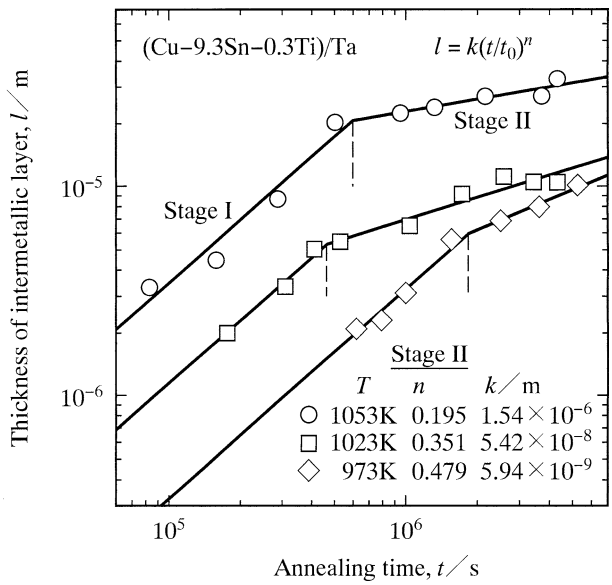

Fig. 5 The mean thickness l of the Ta_9Sn layer versus the annealing time t at $T = 973$, 1023, and 1053 K shown as *open rhombuses*, *squares*, and *circles*, respectively. The *open circles* indicate the result reported in a previous study [21]. The calculations from Eq. 2 are depicted with *straight lines*

$$l = k\left(\frac{t}{t_0}\right)^n. \quad (2)$$

Here, t_0 is unit time, 1 s. It is adopted to make the argument t/t_0 of the power function dimensionless. The proportionality coefficient k has the same dimension as the thickness l, but the exponent n is dimensionless. From the open symbols in Fig. 5, k and n were estimated by the least-squares method in each stage. For stage I, the estimation provides $k = 3.25 \times 10^{-12}$, 1.15×10^{-11}, and 3.47×10^{-11} m at $T = 973$, 1023, and 1053 K, respectively, with $n = 1$. On the other hand, for stage II, the following values are obtained by the estimation: $n = 0.479$ and $k = 5.94 \times 10^{-9}$ m at $T = 973$ K; $n = 0.351$ and $k = 5.42 \times 10^{-8}$ m at $T = 1023$ K; and $n = 0.195$ and $k = 1.54 \times 10^{-6}$ m at $T = 1053$ K. Using these values of n and k, l was calculated as a function of t from Eq. 2. Both results of stages I and II are indicated as solid lines in Fig. 5. The two solid lines at each annealing temperature are intersected each other at $t = t_c$, where t_c is the critical annealing time. The intersection yields $t_c = 1.83 \times 10^6$, 4.63×10^5, and 5.98×10^5 s at $T = 973$, 1023, and 1053 K, respectively. The exponent n is equal to unity at $t < t_c$ but smaller than 0.5 at $t > t_c$. The value of n varies depending on the rate-controlling process for the growth of Ta_9Sn. Hence, the rate-controlling process is dissimilar in stages I and II. The relationship between the rate-controlling process and the exponent n will be discussed in detail later on.

Comparison with growth of Nb_3Sn

The results of $T = 973$, 1023, and 1053 K in Fig. 5 are again shown as open circles with solid lines in Fig. 6a, b, c, respectively. As mentioned in the "Introduction" section, the growth of Nb_3Sn during the reactive diffusion between Nb and the Cu–9.3Sn–0.3Ti alloy was experimentally examined at $T = 923$–1053 K in a previous study [16]. The results of $T = 973$, 1023, and 1053 K for Nb_3Sn are also represented as open squares with dashed lines in Fig. 6a, b, c, respectively. As can be seen, unlike the open circles, the open squares lie well on a single straight line at each annealing temperature. Since n takes values of 0.8–0.7 at $T = 973$–1053 K for Nb_3Sn, the interface reaction as well as the interdiffusion contributes to the rate-controlling process for the growth of Nb_3Sn as discussed later on. Nevertheless, for the growth of Nb_3Sn, the rate-controlling process is independent of the annealing time within the experimental annealing times as reported in a previous study [16].

If the solid line of stage II is extrapolated to the shorter annealing times in stage I, it intersects the dashed line. At the annealing times shorter than the intersection, the growth rate of Ta_9Sn becomes greater than that of Nb_3Sn.

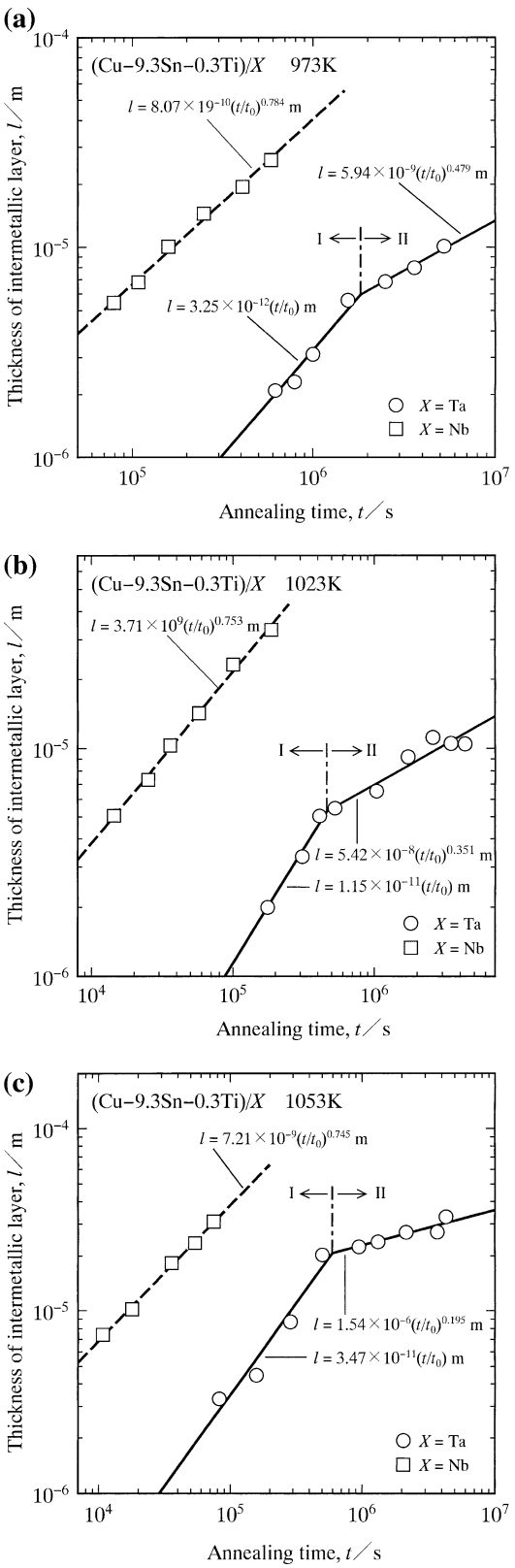

Fig. 6 The results in Fig. 5 are represented as *open circles* with *solid lines* for **a** $T = 973$ K, **b** $T = 1023$ K, and **c** $T = 1053$ K. The corresponding results of Nb_3Sn in a previous study [16] are shown as *open squares* with *dashed lines*

In such a case, Ta is rather quickly consumed by the growth of Ta_9Sn and thus no longer works as the diffusion barrier. Due to the existence of stage I, however, the growth rate during isothermal annealing is practically smaller for Ta_9Sn than for Nb_3Sn.

The exponent n of Ta_9Sn is plotted against the annealing temperature T as open circles and squares for stages I and II, respectively, in Fig. 7. According to the observation with the OM photograph, the Ta_9Sn layer grows mainly toward Ta in the diffusion couple. This means that the growth of Ta_9Sn is predominantly determined by the migration of the Ta_9Sn/Ta interface. When the migration of an interface is controlled by the interface reaction at the migrating interface, n is equal to unity [24]. This is the case of stage I. On the other hand, n is equivalent to 0.5, if the interdiffusion across a growing compound layer is the rate-controlling process for the layer growth and volume diffusion governs the interdiffusion [25]. The value $n = 0.5$ is realized also for the layer growth controlled by boundary diffusion unless grain growth occurs in the compound layer [25]. If grain growth takes place in the compound layer, however, n becomes smaller than 0.5 for the boundary diffusion rate-controlling process. According to the result in Fig. 7, n is smaller than 0.5 for stage II. As T decreases from 1053 to 973 K, n monotonically increases from 0.195 to 0.479. Such dependence of n on T was experimentally observed also for the reactive diffusion between Au and Sn in previous studies [26–28]. In the present study, each polycrystalline grain in the Ta_9Sn layer was not distinguished by the BEI observation. Hence, the metallographical observation of the polycrystalline grain was tried by a chemical-etching technique using various etchants. However, no appropriate etchant was found. Thus, the grain growth of the Ta_9Sn layer could not be detected in a metallographical manner. Nevertheless, we may expect that the same rate-controlling process as the Au–Sn compounds holds for the growth of Ta_9Sn.

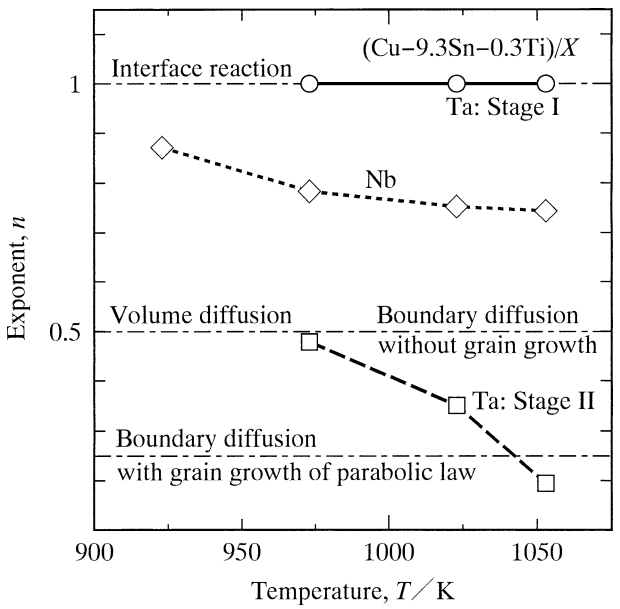

Fig. 7 The exponent n versus the annealing temperature T for stages I and II shown as *open circles* and *squares*, respectively. The corresponding results of Nb_3Sn in a previous study [16] are shown as *open rhombuses*

In Fig. 7, the corresponding results of Nb_3Sn [16] are represented as open rhombuses. In this case, the Nb_3Sn layer grows mainly toward Nb in the diffusion couple. Hence, the migration of the Nb_3Sn/Nb interface primarily determines the growth of the Nb_3Sn layer. The open rhombuses indicate that n is close to unity at $T = 923$ K but decreases to 0.8–0.7 at $T = 973$–1053 K. Therefore, at $T = 923$ K, the migration of the Nb_3Sn/Nb interface is predominantly controlled by the interface reaction at the Nb_3Sn/Nb interface. In contrast, the interdiffusion across the Nb_3Sn layer as well as the interface reaction contributes to the rate-controlling process at $T = 973$–1053 K.

As mentioned earlier, at stage I, the growth of Ta_9Sn is controlled by the interface reaction and thus hardly affected by the diffusion field surrounding Ta_9Sn. In such a case, the growth rate of Ta_9Sn is merely determined by the annealing temperature but independent of the annealing time and the morphology of Ta_9Sn. As a consequence, the result in Fig. 5 can be used to evaluate the consumption rate of the Ta layer sandwiched between the Cu stabilizer and the bronze in the composite-wire during isothermal annealing at stage I. Since no information is available for the crystal structure of Ta_9Sn, it is assumed for the evaluation that the molar volume of Ta_9Sn is equal to that of Ta. If the Ta layer with an initial thickness of $l_{Ta} = 3$ μm is completely consumed to form the Ta_9Sn layer, the Ta_9Sn layer grows to the thickness $l_s = 3.33$ μm. Inserting $l_s = 3.33$ μm into Eq. 2, we obtain $t_s = 1.03 \times 10^6$ s (285 h), 2.91×10^5 s (80.8 h), and 9.61×10^4 s (26.7 h) at $T = 973$, 1023, and 1053 K, respectively. Here, l_s is the thickness of the X–Sn compound layer formed by the complete consumption of the X layer with the initial thickness l_X, and t_s is the annealing time corresponding to $l = l_s$. According to the evaluation, t_s is shorter than t_c at each annealing temperature. Hence, under the present conditions, the growth of Ta_9Sn and the consumption of Ta actually occur at stage I. On the other hand, Nb as well as Ta is used as a diffusion barrier in the bronze method [17–19]. For the growth of Nb_3Sn, however, the interdiffusion and the interface reaction contribute to the rate-controlling process. Therefore, the diffusion field surrounding Nb_3Sn influences the growth rate of Nb_3Sn. Nevertheless, n for Nb_3Sn is much greater than 0.5. Consequently, the influence is still smaller for the growth of Nb_3Sn than for that of the X–Sn compound purely controlled by the interdiffusion. If the molar

volumes of Nb_3Sn and Nb are considered equivalent to each other, the Nb_3Sn layer with a thickness of $l_s = 4$ μm is produced by the complete consumption of the Nb layer with an initial thickness of $l_{Nb} = 3$ μm. As a result, from Eq. 2 with $l_s = 4$ μm, we obtain $t_s = 5.20 \times 10^4$ s (14.4 h), 1.06×10^4 s (2.95 h), and 4.85×10^3 s (1.35 h) at $T = 973$, 1023, and 1053 K, respectively. The values of t_s for Ta and Nb are plotted as open circles and rhombuses, respectively, against the reciprocal of T in Fig. 8. As can be seen, the open symbols lie well on the corresponding straight lines. Therefore, the temperature dependence of t_s is expressed by the following equation:

$$t_s = t_{s0} \exp\left(\frac{Q_t}{RT}\right). \tag{3}$$

Here, t_{s0} is the pre-exponential factor, Q_t is the activation enthalpy, and R is the gas constant. The values of t_{s0} and Q_t were estimated by the least-squares method from the plotted points in Fig. 8. Solid and dashed lines show the estimations for Ta and Nb, respectively. As can be seen, the two lines are almost parallel to each other. However, t_s is about 20 times greater for Ta than for Nb. Thus, the consumption takes place much more sluggishly for Ta than for Nb. If a superconductive compound is formed as a thin layer at the interface between the diffusion barrier and the bronze in the composite-wire, the alternating current (AC) loss of the composite-wire is increased by the thin layer. Unlike Nb_3Sn, Ta_9Sn may not possess superconductivity and hence scarcely increases the AC loss. Consequently, Ta works as a more effective diffusion barrier than Nb. As long as annealing is carried out at $t < t_s$ and Ta remains as a rather uniform layer in the composite-wire, the penetration of Sn into the Cu stabilizer is prevented by the Ta layer.

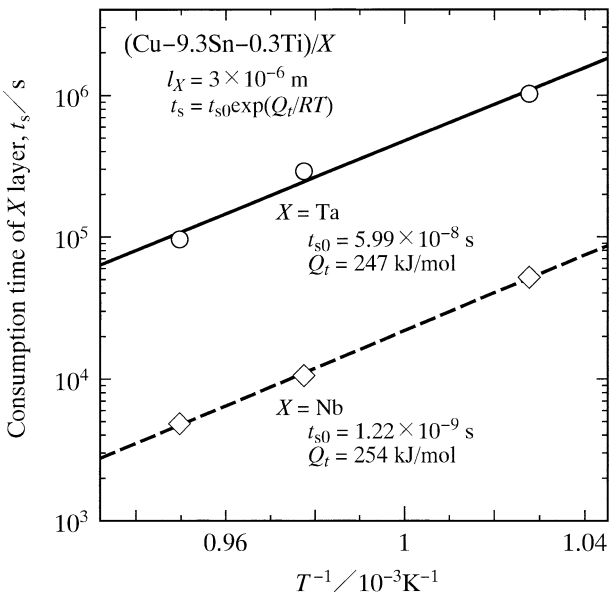

Fig. 8 The consumption time t_s of the X layer with the initial thickness $l_X = 3$ μm versus the reciprocal of the annealing temperature T for X = Ta and Nb shown as *open circles* and *rhombuses*, respectively. *Solid* and *dashed lines* indicate the calculations from Eq. 3 for X = Ta and Nb, respectively

Transition of rate-controlling process

As mentioned in the "Growth behavior of Ta_9Sn" section, the rate-controlling process for the growth of Ta_9Sn varies depending on the annealing time. Such transition of the rate-controlling process is realized also in other solid-state reactions. For instance, the carburization of Fe was experimentally studied by Togashi and Nishizawa [29]. According to their experiment, a layer of the fcc austenite (γ) phase is formed on the bcc ferrite (α) phase of pure Fe and gradually grows into the α phase during isothermal annealing at $T = 1073$ K in an atmosphere with the same activity of C as graphite. Within the experimental annealing times, the growth of the γ phase is controlled by the interface reaction at the migrating γ/α interface in the early stages but by the volume diffusion of C in the α and γ phases in the late stages. Consequently, the transition of the rate-controlling process occurs also for the growth of the γ phase during the carburization of the α phase in the binary Fe–C system. Their experimental result was numerically analyzed using the diffusion equation describing the flux balance of C at the γ/α interface in a previous study [30]. Since the volume diffusion coefficient of C in the γ phase varies depending on the concentration of C [31–35], the composition dependence of the diffusion coefficient was taken into consideration in the numerical analysis. Although no fitting parameter was adopted in the numerical analysis [30], the growth behavior of the γ phase in the late stages was quantitatively explained by the numerical analysis. This means that the growth of the γ phase in the late stages is surely controlled by the volume diffusion.

If l is expressed as a power function of t by Eq. 2 for the growth of a compound layer due to isothermal reactive diffusion in a certain alloy system, the growth rate v of the compound layer is calculated for given values of k and n as follows:

$$v = \frac{\mathrm{d}l}{\mathrm{d}t} = \frac{nk}{t_0}\left(\frac{t_0}{t}\right)^{1-n}. \tag{4}$$

The dependencies of v on t for $n = 1$ and $0 < n \leq 0.5$ evaluated from Eq. 4 are schematically drawn as a horizontal line and a smooth curve, respectively, in Fig. 9. In the case of $n = 1$, Eq. 4 provides $v = k/t_0$, and thus v is constant independent of t. On the other hand, for $0 < n \leq 0.5$, v is infinitely large at $t = 0$ but monotonically decreases with increasing value of t. As a result, the smooth curve intersects the horizontal line at $t = t_c$, where t_c is the critical annealing time as mentioned earlier. Nevertheless, t_c

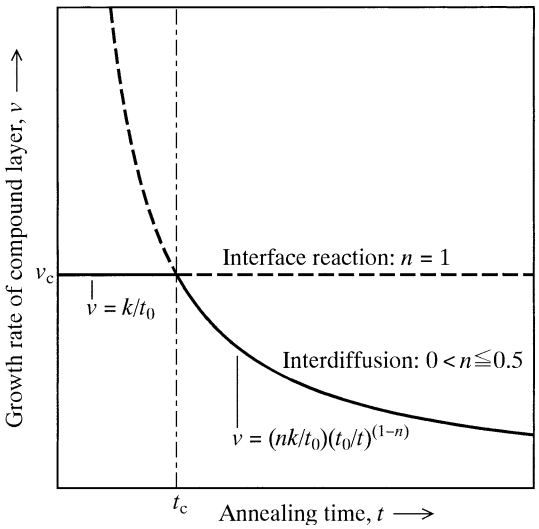

Fig. 9 Schematic relationships for the growth rate v of the compound layer versus the annealing time t obtained from Eq. 4. A *horizontal line* shows the result with $n = 1$, and a *smooth curve* indicates that with $0 < n \leq 0.5$

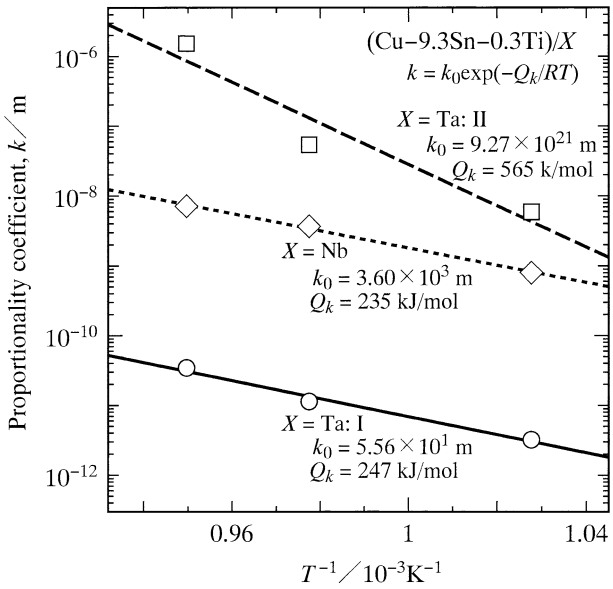

Fig. 10 The proportionality coefficient k versus the reciprocal of the annealing temperature T for stages I and II shown as *open circles* and *squares*, respectively. *Solid* and *dashed lines* indicate the calculations from Eq. 5. The corresponding results of Nb_3Sn in a previous study [16] are shown as *open rhombuses* with a *dotted line*

may not necessarily appear within experimental annealing times. Under realistic experimental conditions, the appearance of t_c depends on the alloy system. As reported in a previous study [36], the growth of the compound layer is determined by the mass transport across the compound layer. In the case of the diffusion rate-controlling process, the mass transport is governed by the interdiffusion. Since the diffusional flux J_i of component i is proportional to the gradient $\Delta\mu_i/l$ of the chemical potential across the compound layer [37], J_i is in inverse relation to l. Here, $\Delta\mu_i$ is the difference between the chemical potentials of component i at the two parallel interfaces sandwiching the compound layer with the thickness l. When the growth of the compound layer proceeds in a semi-infinite diffusion couple, the chemical potential μ_i of component i at each interface remains constant during the growth. Therefore, $\Delta\mu_i$ is also constant independent of t. At $t < t_c$, l is very small, and thus $\Delta\mu_i/l$ is considerably large. In such a case, J_i is large, and hence the growth of the compound layer should be fast. Thus, v may vary depending on t along the dashed curve indicated in Fig. 9. If J_i is very large, however, the interface reaction becomes an obstacle of the interface migration and hence the bottleneck for the growth. As a result, at $t < t_c$, v cannot take infinitely large values but becomes equal to k/t_0 as shown with the solid line in Fig. 9. On the other hand, at $t > t_c$, l is large, and thus $\Delta\mu_i/l$ is relatively small. Under such conditions, J_i is small, and hence the interface reaction is no longer the bottleneck. As a consequence, at $t > t_c$, v varies depending on t along the solid curve indicated in Fig. 9. This is the reason why the growth of the compound layer is controlled by the interface reaction at $t < t_c$ but by the interdiffusion at $t > t_c$.

The values of k for stages I and II are plotted as open circles and squares, respectively, against the reciprocal of T in Fig. 10. The dependence of k on T is usually expressed by the equation [27]

$$k = k_0 \exp\left(-\frac{Q_k}{RT}\right). \tag{5}$$

Here, k_0 is the pre-exponential factor, and Q_k is the activation enthalpy. From the plotted points in Fig. 10, k_0 and Q_k were estimated by the least-squares method for each stage. The estimated values are shown in Fig. 10. Using these values of k_0 and Q_k, k was calculated as a function of T from Eq. 5. The results of stages I and II are shown as solid and dashed lines, respectively, in Fig. 10. As previously mentioned, the interface reaction at the migrating Ta_9Sn/Ta interface is the rate-controlling process for stage I, but the boundary and volume diffusion across the Ta_9Sn layer is that for stage II. As to the interface reaction, the migration rate v of the interface is related with k by the equation $v = k/t_0$. Furthermore, v corresponds to the product of the mobility of the interface and the driving force acting on the interface. Since both the mobility and the driving force vary depending on the temperature, Q_k gives the complex information of their temperature dependencies. Unfortunately, however, no reliable information is available for the thermodynamics of Ta_9Sn and the kinetics of the Ta_9Sn/Ta interface. Consequently, the temperature dependencies of the mobility and the driving force cannot be separately extracted from the value of Q_k

for stage I. The relationship $v = k/t_0 = l_s/t_s$ holds between k and t_s, and both l_s and t_0 are constant. Therefore, Q_t is identical to Q_k for stage I. On the other hand, at stage II, the boundary and volume diffusion contributes to the rate-controlling process, and n varies depending on T. Thus, the complex information of the mixed rate-controlling process is included in the value of Q_k for stage II.

The dependence of k on T for Nb_3Sn at $T = 973$–1053 K reported in a previous study [16] is represented as open rhombuses with a dotted line in Fig. 10. As already shown in Fig. 7, for Nb_3Sn, n slightly decreases with increasing value of T. Such dependence of n on T is included in Q_t. Hence, unlike Ta_9Sn at stage I, Q_t is not exactly equal to Q_k for Nb_3Sn. As mentioned above, the growth of Nb_3Sn is controlled by the interface reaction at the migrating Nb_3Sn/Nb interface as well as the interdiffusion across the Nb_3Sn layer. When the interface reaction is negligible and the boundary diffusion contributes to the interdiffusion, n is smaller than 0.5 as reported in a previous study [25]. If the interface reaction is not negligible, however, n gradually increases with increasing contribution of the interface reaction and may exceed 0.5 under certain conditions. In such a case, the interface reaction masks out the contribution of the boundary diffusion to the interdiffusion [16]. Hence, even for $0.5 < n < 1$, there can be still a possibility that the boundary diffusion contributes to the rate-controlling process. From this point of view, Q_k will include more complex information of the rate-controlling process for Nb_3Sn than for Ta_9Sn. Usually, the rate-controlling process may be estimated from the value of Q_k. If Q_k contains the complex information, however, the rate-controlling process cannot be estimated only from the experimental value of Q_k.

Conclusions

The kinetics of the reactive diffusion between pure Ta and the ternary Cu-9.3 at.% Sn-0.3 at.% Ti alloy was experimentally examined using the sandwich (Cu–Sn–Ti)/Ta/(Cu–Sn–Ti) diffusion couple prepared by a diffusion-bonding technique. The diffusion couple was isothermally annealed in the temperature range between $T = 973$ and 1053 K for various times up to $t = 1462$ h. In this temperature range, the $\alpha + \beta$ two-phase microstructure is realized in the Cu–9.3Sn–0.3Ti alloy. Here, α is the primary solid-solution phase of Cu with the fcc structure, and β is the intermediate phase with the bcc structure. During annealing, the Ta_9Sn layer with a uniform thickness is produced along the initial (Cu–Sn–Ti)/Ta interface in the diffusion couple. The Ta_9Sn layer grows mainly into Ta but scarcely toward the Cu–Sn–Ti alloy. This means that the growth of Ta_9Sn is governed by the migration of the Ta_9Sn/Ta interface. The mean thickness l of the Ta_9Sn layer is expressed as a power function of the annealing time t. The exponent of the power function is equal to unity at $t < t_c$ but smaller than 0.5 at $t > t_c$, where t_c is the critical annealing time. Therefore, the rate-controlling process for the growth of Ta_9Sn varies depending on the annealing time. The interface reaction at the migrating Ta_9Sn/Ta interface is the rate-controlling process at $t < t_c$, but the volume and boundary diffusion across the Ta_9Sn layer is that at $t > t_c$. Since the interface reaction is the bottleneck for the migration of the Ta_9Sn/Ta interface, the growth of Ta_9Sn is sluggish at $t < t_c$. On the other hand, at $t > t_c$, the growth of Ta_9Sn remarkably decelerates due to the exponent smaller than 0.5. As a consequence, during annealing in the bronze method, Ta acts as an effective diffusion barrier against the penetration of Sn into the Cu stabilizer from the bronze in the superconducting Nb_3Sn composite-wire.

Acknowledgements The authors are grateful to Messrs. S. Meguro, K. Wada and H. Sakamoto at Furukawa Electric Co., Ltd., Japan for stimulating discussions. The present study was supported by Furukawa Electric Co., Ltd. The study was also partially supported by a Grant-in-Aid for Scientific Research from the Ministry of Education, Culture, Sports, Science and Technology of Japan.

References

1. Kaufmann AR, Pickett JJ (1970) Bull Am Phys Soc 15:838
2. Suenaga M, Sampson WB (1971) Appl Phys Lett 18:584
3. Tachikawa K, Yoshida Y, Rinderer L (1972) J Mater Sci 7:1154. doi:10.1007/BF00550198
4. Suenaga M, Sampson WB (1972) Appl Phys Lett 20:443
5. Farrell HH, Gilmer GH, Suenaga M (1974) J Appl Phys 45:4025
6. Farrell HH, Gilmer GH, Suenaga M (1975) Thin Solid Films 25:253
7. Dew-Hughes H, Luhman TS, Suenaga M (1976) Nucl Technol 29:268
8. Murase S, Koike Y, Shiraki H (1978) J Appl Phys 49:6020
9. Kwasnitza K, Narlikar AV, Nissen HU, Salathé D (1980) Cryogenics 20:715
10. Upadhyay P, Samanta SB, Narlikar AV (1981) Mater Res Bull 16:741
11. Reddi BV, Raghavan V, Ray S, Narlikar AV (1983) J Mater Sci 18:1165. doi:10.1007/BF00551986
12. Cheng CC, Verhoeven JD (1988) J Less-Com Met 139:15
13. Osamura K, Ochiai S, Kondo S, Namatame M, Nosaki M (1986) J Mater Sci 21:1509. doi:10.1007/BF01114703
14. Muranishi Y, Kajihara M (2005) Mater Sci Eng A 404:33
15. Hayase T, Kajihara M (2006) Mater Sci Eng A 433:83
16. Mikami K, Kajihara M (2007) J Mater Sci 42:8178. doi:10.1007/S10853-007-1700-0
17. Miyahara K, Sumiyoshi F, Funaki K, Iwakuma M, Kubota Y, Ogasawara T, Yamafuji K (1986) Cryogenics 26:234
18. Gislon P, Chiarelli S, Spadoni M, Buttura L, Conti S, Garré R (1995) IEEE Trans Appl Supercond 5:1917
19. McKinnel JC, O'Larey PM, Jablonski PD, Siddall MB (1996) In: Summers LT (ed) Advances in cryogenic engineering, vol 42. Plenum Press, New York, p 1415

20. Courtney TH, Pearsall GW, Wulff J (1965) J Appl Phys 36:3256
21. Kajihara M, Tejima Y (2009) J Phys Conf Ser 165:012091
22. Massalski TB, Okamoto H, Subramanian PR, Kacprzak L (1990) Binary alloy phase diagrams, vol 2. ASM International, Materials Park, Ohio, p 1482
23. Studnitzky T, Schmid-Fetzer R (2002) Z Metallkd 93:894
24. Sutton AP, Balluffi RW (1995) Interfaces in crystalline materials. Oxford Science Publications, Clarendon Press, Oxford, p 603
25. Furuto A, Kajihara M (2008) Mater Trans 49:294
26. Yamada T, Miura K, Kajihara M, Kurokawa N, Sakamoto K (2004) J Mater Sci 39:2327. doi:10.1023/B:JMSC.0000019993.32079.C2
27. Yamada T, Miura K, Kajihara M, Kurokawa N, Sakamoto K (2005) Mater Sci Eng A 390:118
28. Kajihara M, Takenaka T (2007) Mater Sci Forum 539–543:2473
29. Togashi F, Nishizawa T (1976) J Jpn Inst Met 40:12
30. Kajihara M (2009) J Mater Sci 44:2109. doi:10.1007/s10853-009-3299-9
31. Wells C, Batz W, Mehl RF (1950) Trans AIME J Met 188:553
32. Guy AG (1952) Trans Am Soc Met 44:382
33. Smith RP (1953) Acta Metall 1:578
34. Ågren J (1982) Acta Metall 30:841
35. Ågren J (1986) Scr Metall 20:1507
36. Kajihara M (2004) Acta Mater 52:1193
37. Shewmon PG (1963) Diffusion in solids. McGraw-Hill Book Company, New York, p 122